Thermoelectricity of Wigner crystal in a periodic potential

O.V.Zhirov[1,2] and D.L.Shepelyansky[3]

[1] *Budker Institute of Nuclear Physics, 630090 Novosibirsk, Russia*
[2] *Novosibirsk State University, 630090 Novosibirsk, Russia*
[3] *Laboratoire de Physique Théorique du CNRS (IRSAMC), Université de Toulouse, UPS, F-31062 Toulouse, France*

PACS 84.60.Rb – Thermoelectric, electrogasdynamic and other direct energy conversion
PACS 72.20.Pa – Thermoelectric and thermomagnetic effects
PACS 73.20.-r – Electron states at surfaces and interfaces

Abstract –We study numerically the thermoelectricity of the classical Wigner crystal placed in a periodic potential and being in contact with a thermal bath modeled by the Langevin dynamics. At low temperatures the system has sliding and pinned phases with the Aubry transition between them. We show that in the Aubry pinned phase the dimensionless Seebeck coefficient can reach very high values of several hundreds. At the same time the charge and thermal conductivity of crystal drop significantly inside this phase. Still we find that the largest values of ZT factor are reached in the Aubry phase even if for the studied parameter range we obtain $ZT < 2$. We argue that this system provides an optimal regime for reaching high ZT factors and realistic modeling of thermoelecriticy. Possible experimental realizations of this model are discussed.

Introduction. – Computer microelectronic elements go to nanoscale sizes and control of electrical currents and related heat flows becomes a technological challenge (see e.g. [1, 2]). By the thermoelectric effect a temperature difference ΔT generates an electrical current that can be compensated by a voltage difference ΔV. The ratio $S = \Delta V/\Delta T$ is known as the Seebeck coefficient, or thermopower, which plays an important role in the thermoelectric material properties. The thermoelectric materials are ranked by a figure of merit factor $ZT = S^2\sigma T/\kappa$ [3], where σ is the electric conductivity, T is material temperature and κ is the thermal conductivity. To be competitive with usual refrigerators one needs to find materials with $ZT > 3$. Various experimental groups try to reach this high value by skillful methods trying to reduce the thermal conductivity κ of samples keeping high electron conductivity σ and high S (see e.g. [4, 5], [6, 7], [8]). At room temperature the maximal values $ZT \approx 2.4$ have been reached in semiconductor superlattices [4] while for silicon nanowires a factor $ZT \approx 1$ has been demonstrated [5, 6]. This shows that the volume reduction allows to decrease the thermal conductivity of lattice phonons and increase ZT values.

It is interesting to consider the situations when the contribution of lattice phonons is completely suppressed to see if in such a case one can obtain even larger ZT factors. Such extreme regime can be realized with an electron gas, e.g. in two dimensions (2DEG), where at $T \sim 1K$ a contribution of lattice phonons is completely suppressed. In such a regime recent experiments [9] reported giant Seebeck coefficients $S \sim 30mV/K$ obtained in a high resistivity domain.

While it is challenging to eliminate the contribution of lattice phonons experimentally it is rather easy to realize such a situation in numerical simulations simply replacing a lattice of atoms by a fixed periodic potential. After that we are faced the problem of thermoelectricity of Wigner crystal in a periodic potential. In this Letter we study this problem in one dimension (1D), which can be viewed as a mathematical model of silicon nanowires. We note that the ground state and low temperature properties of this system in classical and quantum regimes have been investigated in [10]. It has been shown that at a typical incommensurate electron density the Wigner crystal slides easily in a potential of weak amplitude while above a critical amplitude the electrons are pinned by a lattice. The results [10] show that the properties of the Wigner crystal are similar to those of the Frenkel-Kontorova model where the transition between sliding and pinned phases is known as the Aubry transition [11] (see detailed description in [12]). The positions of electrons on a periodic lattice are locally described by the Chirikov standard map [13, 14]. Similar dynamical properties appear also for the Wigner crystal in wiggling snaked nanochannels [15].

The previous studies of the Wigner crystal in a periodic potential [10] have been concentrated on analysis of the ground state properties at lower temperatures. Here we analyze the transport properties of the crystal at finite temperatures studying its electron and thermal conductivities. Our approach allows to obtain the Seebeck coefficient and the figure of merit ZT at different regimes and various parameters. We note that there has been a significant interest to the heat transport and thermal conductivity in nonlinear lattices [16, 17] but till present there have been no studies of thermoelectricity of interacting electrons in periodic lattices. We present the investigations of this generic case in this Letter.

Model description. – The Hamiltonian of the 1D Wigner crystal in a periodic potential reads:

$$H = \sum_i \left(\frac{p_i^2}{2} + K\cos x_i + \frac{1}{2}\sum_{j\neq i} \frac{1}{|x_i - x_j|} \right), \quad (1)$$

where x_i, p_i are coordinate and momentum of electron i, K is an amplitude of periodic potential or lattice. As in [10] we use the units with $e = m = k_B = 1$, where e and m are electron charge and mass, k_B is the Boltzmann constant, the lattice period is 2π. The rescaling back to physical units is given in [10]. It is interesting to note that at $e = k_B = 1$ we have S as a dimensionless coefficient, e.g. $S = 30mV/K$ from [9] corresponds to $S = 2585$. Generally, in an ergodic regime induced by a developed dynamical chaos or thermal bath, one expects to have $S \sim 1$ since a variation of potential or temperature should produce approximately the same charge redistribution. Thus, in our opinion, large values of dimensionless Seebeck coefficient S indicate a strongly nonergodic regime of system dynamics. We will see below confirmations of this statement.

We concentrate our studies on a case of typical irrational electron density $n_e = \nu/2\pi$, per lattice period, given by the golden rotation number $\nu = \nu_g = 1.618....$ As in [10] we use the Fibonacci rational approximates with N electrons ($0 \leq i \leq N-1$) on M lattice periods (e.g. 34 and 21 or 55 and 34).

According to [10] the Aubry transition at density ν_g takes place at $K = K_c = 0.0462$ so that the Wigner crystal is in a sliding phase for $K < K_c$ and it is pinned by the potential at $K > K_c$. In the latter case there are exponentially many static configurations being exponentially close in energy to the Aubry cantori ground state. The sliding phase corresponds to the continuous Kolmogorov-Arnold-Moser (KAM) curves with ν_g rotation number.

To study the thermoelectic effect in system (1) we add interactions with a substrate, which plays a role of a thermal bath with a given temperature distribution $T(x)$ along x-axis of the electron chain. We also add a static electric field E_{dc}. The thermal bath is modeled by the Langevin force (see e.g. [16]) so that the equations of electron motion take the form:

$$\dot{p}_i = -\partial H/\partial x_i + E_{dc} - \eta p_i + g\xi_i(t)\ , \quad \dot{x}_i = p_i\ . \quad (2)$$

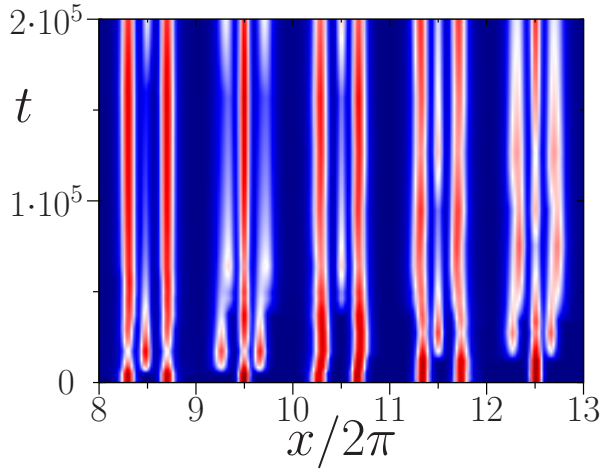

Fig. 1: Electron density variation in space and time from one Langevin trajectory at $K = 2.6K_c$, $T = 0.11K_c$, $\eta = 0.02$, $N = 34$, $M = L/2\pi = 21$; density changes from zero (dark blue) to maximal density (dark red); only a fragment of x space is shown.

Here, the parameter η phenomenologically describes dissipative relaxation processes, and the amplitude of Langevin force is given by the fluctuation-dissipation theorem $g = \sqrt{2\eta T}$. The normally distributed random variables ξ_i are as usually defined by correlators $\langle\langle \xi_i(t)\rangle\rangle = 0$, $\langle\langle \xi_i(t)\xi_j(t')\rangle\rangle = \delta_{ij}\delta(t-t')$. The time evolution is obtained by the 4th order Runge-Kutta integration with a time step Δt, at each such a step the Langevin contribution is taken into account. We checked that the results are not sensitive to the step Δt by its variation by a factor ten, the data are mainly obtained with $\Delta t = 0.02$. We use the hard wall boundary conditions for electrons at the ends of the chain $x = 0; L$ with the total system length $L = 2\pi M$. We also note that the Coulomb interaction couples all electrons in the sample. However, the results of [10, 15] show that only nearest neighbors are effectively count. Due to that we present the numerical results for this approximation. We ensured that our results are not sensitive to including other neighbors.

A typical variation of electron density in space x and time t is shown in Fig. 1 for the Aubry pinned phase. Transitions, induced by thermal fluctuations, from one to two electrons inside one potential minimum are well visible.

Numerical results for Seebeck coefficient. – To compute S we impose a constant temperature gradient on the Langevin substrate with a temperature difference ΔT at the sample ends. Then we compute the local electron temperature $T_e(x) = \langle p^2(x)\rangle_t$ where the time average of electron velocities are done over a large time interval with up to $t = 10^7$. To eliminate periodic oscillations along the chain we divide it on M bins of size 2π and do all averaging inside each bin. Typical examples of variations of

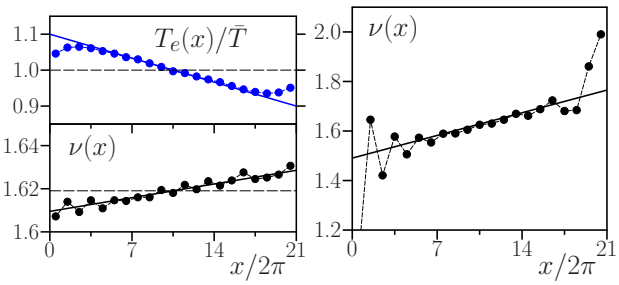

Fig. 2: *Left panels*: dependence of electron temperature $T_e(x)$ *(top, blue points)* and rescaled density $\nu(x)$ *(bottom, black points)* on distance x along the chain placed on the Langevin substrate with a constant temperature gradient (it is shown by the blue line) at average temperature $\bar{T} = 0.01$ and temperature difference $\Delta T = 0.2\bar{T}$; black line shows the fit of density variation in the bulk part of the sample. *Right panel*: density variation produced by a static electric field $E_{dc} = 4 \times 10^{-4}$ at a constant substrate temperature $T = 0.01$; black line shows the fit of gradient in the bulk part of the sample. Here $N = 34, M = 21$, $K = 1.52K_c$, $\eta = 0.02$, averaging is done over time interval $t = 10^7$; $S = 3.3$ at $T = 0.01 \approx 0.22K_c$

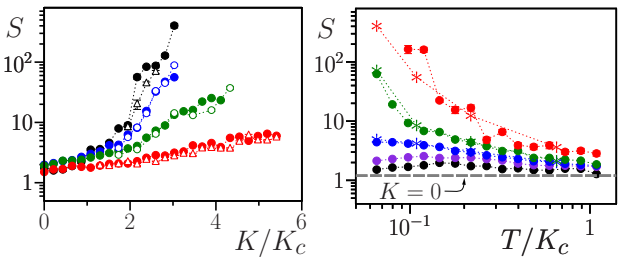

Fig. 3: *Left panel*: Dependence of the Seebeck coefficient S on rescaled potential amplitude K/K_c at temperatures $T/K_c = 0.065, 0.11, 0.22$ and 0.65 shown by black, blue, green and red colors, respectively from top to bottom. The full and open symbols correspond respectively to chains with $N = 34$, $M = 21$ and $N = 55$, $M = 34$. *Right panel*: Dependence of S on T/K_c at different $K/K_c = 0, 0.75, 1.5, 2.2, 3$ shown respectively by black, violet, blue, green and red points; $N = 34$, $M = 21$; the dashed gray line shows the case $K = 0$ for noninteracting particles. The stars show corresponding results from left plane at same N, M. Dotted curves are drown to adapt an eye. Here and in other Figs. the statistical error bars are shown when they are larger than the symbol size. Here $\eta = 0.02$.

electron temperature $T_e(x)$ and electron rescaled density $\nu(x) = 2\pi n_e(x)$ along the chain are shown for a given ΔT in Fig. 2 (left panels). The chain ends are influenced by the boundary conditions, but in the main bulk part of the sample we obtain a linear gradient variation of $T_e(x)$ and $\nu(x)$. The linear fit of $T_e(x)$ and $\nu(x)$ in the bulk part allows to determine the response of the Wigner crystal on substrate temperature variation. In a similar way at fixed substrate temperature T we can find the density variation $\nu(x)$ induced by a static field E_{dc} at the voltage difference $\Delta V = E_{dc}L$, as it is shown in Fig. 2 (right panel). For the computation of S we find convenient to apply such a voltage ΔV which at fixed T creates the same density gradient as those induced by temperature difference ΔT at $E_{dc} = 0$. Then by definition $S = \Delta V/\Delta T$. The data are obtained in the linear response regime when $\Delta T, E_{dc}$ are sufficiently small.

The dependencies of obtained Seebeck coefficient S on K and T are presented in Fig. 3. The data show that at $K < K_c$ we have $S \sim 1$ practically for all temperatures. Here the Lanvegin thermostat efficiently produce ergodic distribution over all configurations of electrons and we have $S \sim 1$ in agreement with the above ergodic argument. For $K > K_c$ we find a significant increase of S at low temperatures $T < K_c$. In this regime the crystal is pinned by the lattice and different configuration states are separated by potential barriers $\Delta U \sim K - K_c$ so that the transitions between configurations are suppressed by the Boltzmann factor $\exp(-\Delta U/T)$. Thus here long times are needed to have a transition between configurations [10]. In such a regime large voltage ΔV is required to produce the same density gradient as those given by a fixed ΔT. This leads to large S values generated by big and rare thermal fluctuations.

To check the stability of obtained results in the nonergodic regime with large S we use three different numerical methods:

(a) *cold start* from the Aubry ground state at a given K and $T = 0$, followed by a warm up to required T and then computing of the responses to a temperature gradient or electric field; in this approach the system evolves during a relaxation time $t_{rel} \sim 10^6$ until the density response is stabilized, then the computations of gradients are performed on a time scale t_{com} determined by the condition of target statistical accuracy (typically $t_{com} \sim 10^7$);

(b) *zero potential start* from the ground state at $K = 0$ and given T followed by a sweep over K with a step ΔK (typically $\Delta K = 0.01$); at each step the responses of current state to E_{dc} or ΔT are determined; after $t_{rel} = 5\times10^4$ the gradients are computed on times $t_{com} \geq 10^4$ determined by target accuracy; next step to $K + \Delta K$ starts from the reached steady state at previous K value, continuing up to required K_{max} value complete one sweep in K; then we repeat sweeps about 20 to 100 times to improve statistical accuracy;

(c) *hot start* from the Aubry ground state at given K with a warm up to $T_{max} = 0.05 \approx K_c$, followed by a sweep from $T = T_{max}$ down to $T = T_{min} = 0.003$ with equidistant steps in $\ln T$, in a way similar to (b) with a similar number of sweeps.

The data in left and right panels of Fig.3 are obtained by the methods (b) and (c) respectively. The stars in the right panel show the corresponding data from the left plane. A good agreement between methods (b) and (c) confirms the validity of obtained results. The results from a more time-consuming method (a) give a similar agreement with

those methods (b),(c) of Fig. 3 (data not shown). The comparison of results with $N = 34$ and 55 electrons shows their independence of the chain length. However, at $K \gg K_c$ and $T \ll K_c$ very long computations are required to obtain statistically reliable results.

The obtained results show that large values of $S > 100$ can be reached in the pinned phase $K > K_c$ at low temperatures. The growth of S is roughly proportional to the inverse Boltzmann factor. This nonergodic regime is characterized by big fluctuations. We think that a similar regime appeared in 2DEG experiments with even larger values $S \sim 10^3$ [9].

Properties of charge and thermal conductivities. – The large values of S do not guaranty high values of figure of merit factor ZT which depends also on charge and thermal conductivities σ, κ.

To determine σ we use the periodic boundary conditions and compute the average velocity v_{el} of the Wigner crystal in a weak electric field E_{dc} being in a linear response regime. The averaging is done over a typical time interval $t = 10^7$ and over all electrons. Then the charge current is $j = n_e v_{el} = \nu v_{el}/2\pi$ and $\sigma = j/E_{dc}$. In absence of potential at $K = 0$ we have a crystal moving as a whole with $v_{el} = E_{dc}/\eta$ and corresponding to the conductivity $\sigma = \sigma_0 = \nu_g/(2\pi\eta)$ ($\nu_g \approx 1.618...$). This theoretical result is well reproduced by numerical simulations as it is shown in Fig. 4 (left panel).

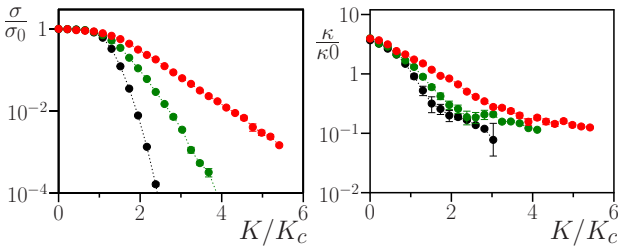

Fig. 4: *Left panel*: Rescaled electron conductivity σ/σ_0 as a function of K/K_c shown at rescaled temperatures $T/K_c = 0.065$, 0.22, 0.65 by black, green and red points respectively. *Right panel*: Rescaled thermal conductivity κ/κ_0 as a function of K/K_c shown at same temperatures and colors as in left panel. Here we have $N = 34$, $M = 21$, $\eta = 0.02$, $\sigma_0 = \nu_g/(2\pi\eta)$, $\kappa_0 = \sigma_0 K_c$.

For $K < K_c$ the conductivity σ is practically independent of T, K. However, for $K > K_c$ we have a sharp exponential drop of σ with increasing K and decreasing temperature. This drop is satisfactory described by the thermal activation dependence $\sigma \propto \exp(-(K-K_c)/T)$, at least when K is significantly larger K_c. We note that the temperature dependence differs significantly from those in 2DEG experiments [9] where resistivity becomes independent of T for $T < 1K$. We attribute this to 2D features of these experiments and to quantum effects being important at $T \sim 1K$. Indeed, the quantum fluctuations can produce sliding of the Wigner crystal even in the classically pinned phase as it is shown for 1D in [10].

Another important feature of σ variation with the system parameters is that $\sigma \sim 1/\eta$ for $K < K_c$ and that σ is practically independent of η for $K > K_c$. We will discuss this point in more detail later.

The thermal gradient produces not only the charge density variation but also a heat flow J. This flow is related to the temperature gradient by the Fourier law with the thermal conductivity κ: $J = \kappa \partial T/\partial x$ (see e.g. [2,16]). The flow J can be determined from the analysis of forces acting on a given electron i from left and right sides respectively: $f_i^L = \sum_{j<i} 1/|x_i - x_j|^2$, $f_i^R = -\sum_{j>i} 1/|x_i - x_j|^2$. The time averaged energy flows, from left and right sides, to an electron i moving with a velocity v_i are respectively $J_{L,R} = \langle f_i^{L,R} v_i \rangle_t$. In a steady state the mean electron energy is independent of time and $J_L + J_R = 0$. But the difference of these flows gives the heat flow along the chain: $J = (J_R - J_L)/2 = \langle (f_i^R - f_i^L) v_i/2 \rangle_t$. This computation of the heat flow, done with hard wall boundary conditions, allows us to determine the thermal conductivity via the relation $\kappa = JL/\Delta T$.

In principle, each electron interacts also with the substrate. However, in the central part of the chain the electron temperature is equal to the local temperature of the substrate due to local thermal equilibrium. This fact is directly seen in Fig. 2 (left top panel, *cf.* blue points and straight line). Thus, we perform additional averaging of the heat flow in the central 1/3 part of the chain improving the statistical accuracy of data.

The dependence of computed thermal conductivity κ on the amplitude of the potential K is shown in Fig. 4 (right panel). It is convenient to present κ via a ratio to $\kappa_0 = \sigma_0 K_c$ to have results in dimensionless units. Similar to the charge conductivity σ, we find that $\kappa \approx 3.9\kappa_0$ at $K < K_c$ being practically independent of temperature T. However, the transition to zero temperature and $\eta = 0$ is singular due to divergence of κ in weakly nonlinear regular chains as discussed in [16].

In the pinned phase at $K > K_c$ we see an exponential drop of κ with increase of K and decrease of T at $T < K_c$. As for σ, we find that for $K > K_c$ the thermal conductivity is practically independent of dissipation rate η. We will discuss this in more detail below.

Results for figure of merit factor ZT. – Now we determined all required characteristics and can analyze what ZT values are typical for our system and how ZT depends on the parameters.

The main results are presented in Fig. 5. They show that in our system we have $ZT \leq 2$. At fixed T we have an optimal value of K with a maximum of ZT at a certain $K \sim 2K_c$, its position moves slightly to larger K with an increase of T (left panels). At fixed $K = 2.6K_c$, taken approximately at the maximum of ZT (left bottom panel). There is a visible increase of ZT with increasing T approximately by a factor 3 in a range $0.1 \leq T/K_c \leq 1$

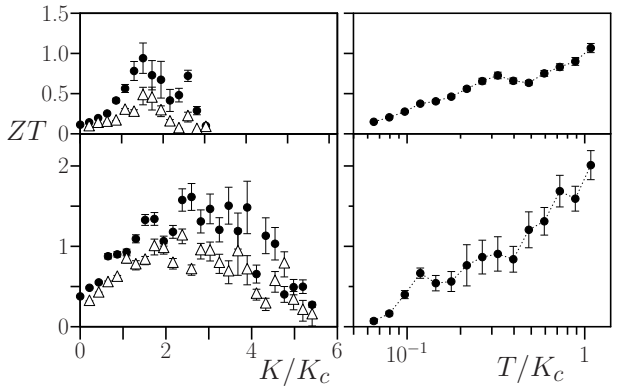

Fig. 5: *Left panels*: Dependence of ZT on K/K_c at temperatures $T/K_c = 0.11$ (top panel) and $T/K_c = 0.65$ (bottom panel); the black points and open triangles correspond respectively to $\eta = 0.02$ and $\eta = 0.05$. *Right panels*: Dependence of ZT on T/K_c for $K/K_c = 0.75$ (top panel) and $K/K_c = 2.6$ (bottom panel) at $\eta = 0.02$. In all panels $N = 34$, $M = 21$.

(right panels). A further increase up to $T \gg K_c$ is not very interesting since then we come to the case without lattice where ZT is small.

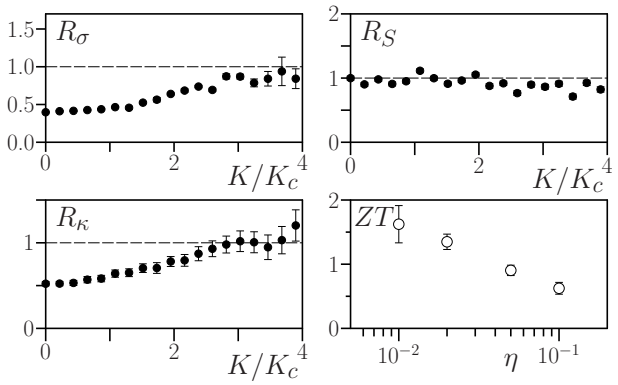

Fig. 6: *Left panels*: Dependence of ratios R_σ (top) and R_κ (bottom) on K/K_c at $T/K_c = 0.65$. *Right top panel*: Same as in left panels for ratio R_S. All ratios are defined in the text. *Right bottom panel*: dependence of ZT on η at $T/T_c = 0.65$; ZT values are averaged over interval $2.1 < K/K_c < 3.1$. Here $N = 34$, $M = 21$.

The results for two values of dissipation $\eta = 0.02; 0.05$ shown in Fig. 5 indicate that ZT drops with increase of η. To understand the effects of η in a better way we show the dependence of ratio $R_S = S(\eta = 0.05)/S(\eta = 0.02)$ on K/K_c at fixed $T/K_c = 0.65$ in Fig. 6. The dependence of similar ratios R_σ and R_κ for σ and κ are also shown there. We find $R_\sigma \approx R_\kappa \approx 0.5$ at $K \ll K_c$ and $R_\sigma \approx R_\kappa \approx 1$ for $K > K_c$. At $K \ll K_c$ the ratios are close to the expected value 0.4 following from the theoretical scaling $\sigma_0 \propto 1/\eta$ and similar expected dependence $\kappa_0 \propto 1/\eta$. However, in the pinned phase the dependence of σ and κ on η practically disappears. The physical mechanism of this effect is due to the fact that the electrons are pinned by the lattice and Wigner crystal phonons are localized, and hence, their mean free path becomes smaller than its value at $K = 0$ when it is given by the dissipative exchange with the Langevin substrate. The ratio R_S is not sensitive to the variation of K/K_c even if S changes strongly with K (see Fig. 3). A similar behaviour of ratios is obtained at lower $T/K_c \approx 0.1$ with somewhat more sharp change between limit values 0.5 and 1 around $K/K_c \approx 2$. We also checked that the ratios constructed for other values of η (e.g. $\eta = 0.01, 0.1$, instead of above $\eta = 0.05$) also saturate at unit value for $K/K_c > 2$. Thus, at $K/K_c > 2$, the localization effects, induced by pinning, dominate over mean free path at $K = 0$.

The dependence of ZT on η is also shown in Fig. 6. We see that a decrease of η generates a slow growth of ZT even if at so low value as $\eta = 0.01$ we still have $ZT < 2$. Here, we give numerical values of η in our computational units. It is more physical to look of a dimensionless ratio η/ω_0 where ω_0 is a maximal frequency of small oscillations near a vicinity of the Aubry ground state at $K = K_c$. According to the results [10] we have $\omega_0 \approx 2\sqrt{K_c} \approx 0.41$. Thus all our data are obtained in the regime of long relaxation time scale ($\eta/\omega_0 \ll 1$).

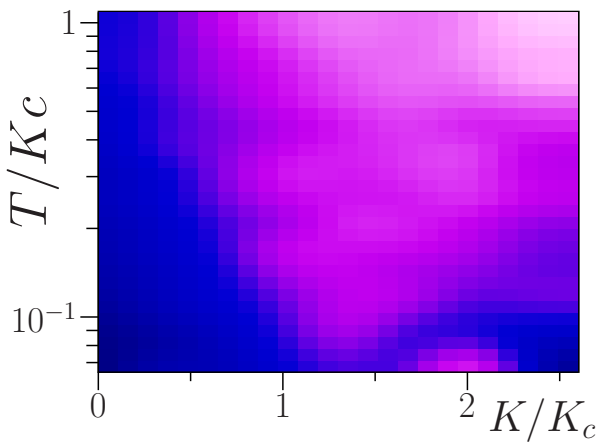

Fig. 7: Dependence of ZT on K/K_c and T/K_c shown by color changing from $ZT = 0$ (dark blue) to maximal $ZT = 1.92$ (light rose). Here $\eta = 0.02$, $N = 34$, $M = 21$.

The global dependence of ZT on K/K_c and T/K_c is presented in Fig. 7 for the investigated parameter range. The maximal value $ZT \approx 1.9$ is reached at $K/K_c \approx 2.6$ and $T/K_c \approx 1.1$. It is possible that ZT values may be higher at $K > 2.6K_c$ and $T > K_c$. However, at so large K and T the transitions between different minima fluctuate strongly and also there appear close encounters between electrons and hence, the integration step should be significantly reduced. Therefore, this range requires even more detailed and advanced numerical simulations.

Discussion. – Our studies of the Wigner crystal in a periodic potential show that in the Aubry pinned phase at

$K > K_c$ the Wigner crystal has very larger Seebeck coefficients S which grow exponentially with a decrease of temperature or increase of the potential amplitude. However, at the same time the charge and thermal conductivities drop significantly. As a result, for the all variety of cases studied we obtain the maximal value of $ZT \leq 2$. Thus, there is a rather nontrivial compensation of three quantities S, σ, κ which determine the figure of merit, ZT. In global, the pinned phase has larger ZT values, compared to the sliding phase at $K < K_c$. Hence, there are hopes to reach even larger ZT in this pinned phase at optimized system parameters. We find that ZT weakly increases with a decrease of the seed relaxation rate η. Thus a further decrease of η may allow to reach $ZT > 3$. However, special efforts should be performed to determine this seed η for real materials since in the pinned phase the charge and thermal conductivities drop significantly, compared to the sliding phase, becoming practically independent of seed relaxation rate.

It is also possible that further temperature increase significantly above $T > K_c$ may produce $ZT > 3$. However, the growth of ZT with T is slow, being close to logarithmic growth, so that such high T may be not interesting in practice. We also note that at large K and T the accuracy of numerical integration should be improved significantly due to close encounters between electrons.

Thus the task to reach $ZT > 3$ seems to be hard even in our simple model where the thermal conductivity of atomic lattice phonons is eliminated from the beginning and only electronic conductivity contribution is left. In this sense our model provides a superior bound for ZT factor in 1D. We expect that for the Wigner crystal in two- and three-dimensional potentials the factor ZT will be reduced, compared to 1D case, since it will be more difficult to localize phonons of Wigner crystal. Thus, in a certain sense we expect that our model provides the most optimal conditions for large ZT values and still we remain at $ZT < 2$. Hence, further investigations are required.

Finally we provide some physical values of our model parameters. In physical units we can estimate the critical potential amplitude as $U_c = K_c e^2/(\epsilon d)$, where ϵ is a dielectric constant, Δx is a lattice period and $d = \nu \Delta x/2\pi$ is a rescaled lattice constant [10]. For values typical for a charge density wave regime [18] we have $\epsilon \sim 10$, $\nu \sim 1$, $\Delta x \sim 1nm$ and $U_c \sim 40mV \sim 500K$ so that the Aubry pinned phase should be visible at room temperature. The obtained U_c value is rather high that justifies the fact that we investigated thermoelectricity in the frame of classical mechanics of interacting electrons. In any case the real thermoelectric devices should work at room temperature and in this regime the classical treatment of electron transport can be considered as a good first approximation.

We think that it would be useful to perform experimental studies of electron transport in a periodic potential. We hope that such type of experiments can be possible with charge density waves (see e.g. [18] and Refs. therein), strongly interacting electrons in ultraclean carbon nanotubes with interaction energies of $100mV$ [19], experiments with electrons on a surface of liquid helium [20], and cold ions in optical lattices [21].

The research of OVZ was partially supported by the Ministry of Education and Science of Russian Federation.

REFERENCES

[1] Majumdar A., *Science*, **303** (2004) 777.
[2] Goldsmid H.J., *Introduction to thermoelectricity* (Springer, Berlin) 2009.
[3] Ioffe A.F. and Syil'bans L.S., *Rep. Prog. Phys.*, **22** (1959) 167.
[4] Venkatasubramanian R. *et al.*, *Nature*, **413** (2001) 597.
[5] Hochbaum A.I. *et al.*, *Nature*, **451** (2008) 163.
[6] Boukai A.I. *et al.*, *Nature*, **451** (2008) 168.
[7] Poudel B. *et al.*, *Science*, **320** (2008) 634.
[8] Biswas K. *et al.*, *Nature*, **489** (2012) 414.
[9] Narayan V. *et al.*, *Phys. Rev. B*, **86** (2012) 125406.
[10] Garcia-Mata I., Zhirov O.V. and Shepelyansky D.L., *Eur. Phys J. D*, **41** (2007) 325.
[11] Aubry S., *Physica D*, **7** (1983) 240.
[12] Braun O.M. and Kivshar Yu.S., *The Frenkel-Kontorova model: concepts, methods, applications* (Springer-Verlag, Berlin) 2004.
[13] Chirikov B.V., *Phys. Rep.*, **52** (1979) 263.
[14] Chirikov B.V. and Shepelyansky D.L., *Scholarpedia*, **3(3)** (2008) 3550.
[15] Zhirov O.V. and Shepelyansky D.L., *Eur. Phys J. B*, **82** (2011) 63.
[16] Lepri S., Livi R. and Politi A., *Phys. Rep.*, **377** (2003) 1.
[17] Li N. *et al.*, *Rev. Mod. Phys.*, **84** (2012) 1045.
[18] Brazovskii S. *et al.*, *Phys. Rev. Lett.* , **108** (2012) 096801.
[19] Deshpande V.V *et al.*, *Science*, **323** (2009) 106
[20] Rees D.G. *et al.*, *Phys. Rev. Lett.* , **106** (2011) 026803.
[21] Pruttivarasin T. *et al.*, *New J. Phys.*, **13** (2011) 075012.